Open

LABORATORY SCIENCE

Halo assessment in intraocular lenses through high dynamic range images

Clara García-Pedreño, MSc, Juan Tabernero, PhD, Harilaos Ginis, PhD, Lucía Hervella, PhD, Pablo Artal, PhD

Purpose: To analyze the halo formation of several intraocular lenses (IOLs) in the optical bench.

Setting: University of Murcia, Murcia, Spain.

Design: In vitro study.

Methods: Light from a green LED passed through a pinhole and was collimated. Each IOL was placed within a realistic model eye having a PMMA cornea with a physiological amount of spherical aberration and a 4.5 mm aperture. A digital camera sensor acted as the retina and a focus tunable lens was used to change the object's vergence (range ±4 diopters). Series of images were captured with different exposure times and fused to get a high dynamic range image. Performance was assessed by analyzing the corresponding halo brightness and size. The tested lenses, that included biconvex and inverted meniscus IOLs, were monofocals, extended depth-of-focus (EDOF), and diffractive trifocals.

Results: Monofocal lenses produced halos with a radius close to 0.4 degrees. The halo radii of the nondiffractive EDOF lenses ranged between 0.45 and 0.63 degrees, whereas diffractive lenses had radii ranging from 0.84 to 1.22 degrees. The halo was generally dimmer for the refractive lenses and brighter for the diffractive. The through-focus images show that the halo size was larger at any defocus position for the diffractive lenses than for the rest of the tested IOLs.

Conclusions: The diffractive IOLs exhibited a characteristic halo structure. Performance of the inverted meniscus and other nondiffractive lenses (Vivity and Eyhance) was comparable with a monofocal lens. This on-bench test can serve as an indication of the potential impact of photic phenomena on patient satisfaction.

J Cataract Refract Surg 2026; 52:296–302 Copyright © 2026 The Author(s). Published by Wolters Kluwer Health, Inc. on behalf of ASCRS and ESCRS

Intraocular lenses (IOLs) implanted in cataract surgery can create a variety of unwanted visual phenomena such as glare and halos that can be particularly severe for multifocal lenses, both refractive and diffractive, as a consequence of their optical design: The fixed foci create focused and out of focus images in the retina, and the latter might be perceived as halos.[1–4] In the past few years, lens designs that aim to extend the depth of focus instead of creating different foci for specific distances have appeared. These lenses could decrease the appearance of halos associated with the additional powers of multifocal IOLs. Some approaches used for this purpose are increasing the amount of spherical aberration (SA) or other modifications to the lens profile.[5–7] In addition, lenses with an inverted meniscus profile have emerged as an alternative to improve the peripheral optical quality and have also proven to prevent negative dysphotopsias.[8,9]

The incidence of photic phenomena in pseudophakic eyes is usually reported by subjective assessment such as questionnaires or semiobjective methods such as halo and glare simulators, but there is no standard as to how to evaluate them clinically.[10–12] To have an objective criterion to evaluate photic phenomena produced by IOLs, optical bench testing is a good alternative. In the latest ISO 11979-2 and ANSI Z80.35 standards for IOL testing, the measurement of halos on the optical bench has been proposed.[13,14] Previous research has assessed the halo formation in IOLs in vitro and has found good correlation between on-bench testing and patient-reported halos.[4,15] Apart from testing the optical properties, measuring the image quality of the IOLs in vitro can help both patients and doctors make a more informed decision about the best lens to implant.

Thus, the aim of this study was to compare the halo formation in a variety of IOL types, including diffractive trifocals, nondiffractive extended depth-of-focus (EDOF), and inverted meniscus lenses on the optical bench using a physiological model eye. Halo formation was assessed at

Submitted: July 1, 2025 | Final revision submitted: November 27, 2025 | Accepted: December 16, 2025

From the Laboratorio de Óptica, Universidad de Murcia, Murcia, Spain (García-Pedreño, Artal); Voptica SL, Murcia, Spain (García-Pedreño, Ginis, Hervella); Departamento de Electromagnetismo y Electrónica, Universidad de Murcia, Murcia, Spain (Tabernero); Diestia Systems, Athens, Greece (Ginis).

Presented in part at the 42nd Congress of the ESCRS, Barcelona, Spain, September 2024; and at the 2025 ARVO Annual Meeting, Salt Lake City, Utah, May 2025.

This study was supported by the following grants: Agencia Estatal de la Investigación (PID2022-139838OB-I00); grant DIN2024-013367 financed by MICIU/AEI/10.13039/501100011033; FEDER, UE (PID2023-146439OB-I00).

Corresponding author: Clara García-Pedreño, MSc, Centro de Investigación en Óptica y Nanofísica, Universidad de Murcia, 30100, Murcia, Spain. Email: claraisabel.garciap@um.es.

0886-3350/$ - see frontmatter
https://doi.org/10.1097/j.jcrs.0000000000001860

the far focus of the IOLs, allowing comparison of all lenses with a monofocal reference. In addition, halos were evaluated through focus to characterize performance over the visual range provided by each lens, offering a more comprehensive characterization of the EDOF and multifocal lenses.

METHODS

IOLs

Since the study aims to provide a comparison of the performance between IOLs, the intention was to measure a wide variety of lens types, which are described in Table 1. The base power of the lenses ranged from 19 to 22 diopters (D). From the total of 10 lenses that were measured, 3 of them had an inverted meniscus shape and an EDOF design based on negative SA to induce different amounts of depth of focus (ArtIOLs): Art25 can be considered a monofocal plus, Art40 as EDOF, and Art70 as full visual range (FVR).[16,17] The rest of lenses that were tested were 2 monofocal (Tecnis ZCB00, Acriol), an enhanced monofocal (Eyhance), an EDOF with wavefront shaping technology (AcrySof IQ Vivity), and 3 diffractive trifocals (AcrySof IQ PanOptix, AT Lisa Tri 839MP, and FineVision POD F).

Optical Bench Setup

The experimental system is described in Figure 1 and consisted of a green LED (LED528EHP, Thorlabs, Inc.), with λ = 525 nm, λ_{HFW} = 35 nm, illuminating a 200 µm pinhole (P200K, Thorlabs, Inc.), a collimating achromatic lens (f = 100 mm), and a tunable lens (EL-16-40-TC-VIS-20D, Optotune AG) conjugated with the spectacle plane. The model eye is described in more detail elsewhere but is briefly discussed here for clarity.[18,19] A PMMA cornea with physiological dimensions and +0.28 µm of SA (at 5.15 mm aperture in the pupil plane) is followed by a 4.5 mm diameter aperture and the desired IOL placed in a holder. That amount of corneal SA is in good agreement with the average human SA, and pupil size was chosen to simulate mesopic pupils.[20,21] A digital camera sensor (DFM 72BUC02ML, The Imaging Source), protected by a waterproof casing, acted as the retina and could be displaced in the optical axis. The eye was filled with deionized water. Once the IOL was placed in the eye, the camera acting as the retina was manually displaced to find the best far focus and image acquisition started.

Measuring halos requires a wide dynamic range because their intensity is significantly lower than that of the focused spot. To overcome the limited dynamic range of the sensor used (8 bits), this study proposes the creation of high dynamic range (HDR) images by combining images taken at different exposures. Object vergence was varied with the tunable lens from −4 to +4 D in 0.25 D steps. Negative object vergence simulates the object moving closer to the eye. For each vergence, images of the pinhole and background were collected with 5 exposures ranging from 0.1 to 10 milliseconds.

The 2 main deviations from the standard setup commonly used in IOL bench testing were placing the sensor inside the artificial eye rather than recording aerial images outside of it and varying object vergence while keeping the image plane fixed, instead of shifting the image plane for through-focus measurements.[22] These modifications were included to more closely replicate physiological viewing conditions.

Image Analysis

A script in MATLAB (R2022b, The Mathworks, Inc.) was developed to analyze the images. First, the background images were subtracted from the pinhole images to reduce noise. The different exposure images were fused to get HDR images for each object vergence. This process weighs each image according to its exposure time and then averages all of them excluding the underexposed and overexposed pixels, to create a single image with higher dynamic range.[23] In this study, this was achieved using the function *makehdr* from MATLAB's Image Processing Toolbox, using as inputs the desired images and the exposure time of each image.

The equivalence from pixel to degrees of visual angle in the retina was determined considering the sensor pixel size and the posterior nodal distance of the eye (calculated for the base power of each lens). This provided the angular size of a single pixel, referenced to the nodal point, which was then used as the scale for all subsequent analyses. Images were then cropped to 6 degrees of visual angle and converted to grayscale.

For the through-focus analysis, the HDR images of all vergences were stacked in a matrix that was normalized. The radial average

Table 1. Measured Intraocular Lenses and Their Characteristics

IOL	Manufacturer	Power (D)	Category	Optics
ArtIOL Art25	Voptica SL	20	Monofocal plus	Aspheric Inv meniscus
ArtIOL Art40	Voptica SL	20	EDOF	Aspheric Inv meniscus
ArtIOL Art70	Voptica SL	20	EDOF/FVR	Aspheric Inv meniscus
Acriol	Care Group	20	Monofocal	Aspheric
Tecnis ZCB00	Johnson & Johnson Vision	20	Monofocal	Aspheric
Tecnis Eyhance ICB00	Johnson & Johnson Vision	19	Enhanced monofocal	Aspheric Continuous power profile
AcrySof IQ Vivity	Alcon Laboratories, Inc.	20	EDOF	Aspheric Wavefront shaping
AcrySof IQ TFNT00 (PanOptix)	Alcon Laboratories, Inc.	20 (+2.2 and +3.2)	Trifocal	Aspheric Diffractive
AT LISA Tri 839MP	Carl Zeiss Meditech AG	22 (+1.66 and +3.33)	Trifocal	Aspheric Diffractive
FineVision POD F	Beaver-Visitec International (PhysIOL)	22 (+1.75 and +3.5)	Trifocal	Aspheric Diffractive

EDOF = extended depth-of-focus; FVR = full visual range

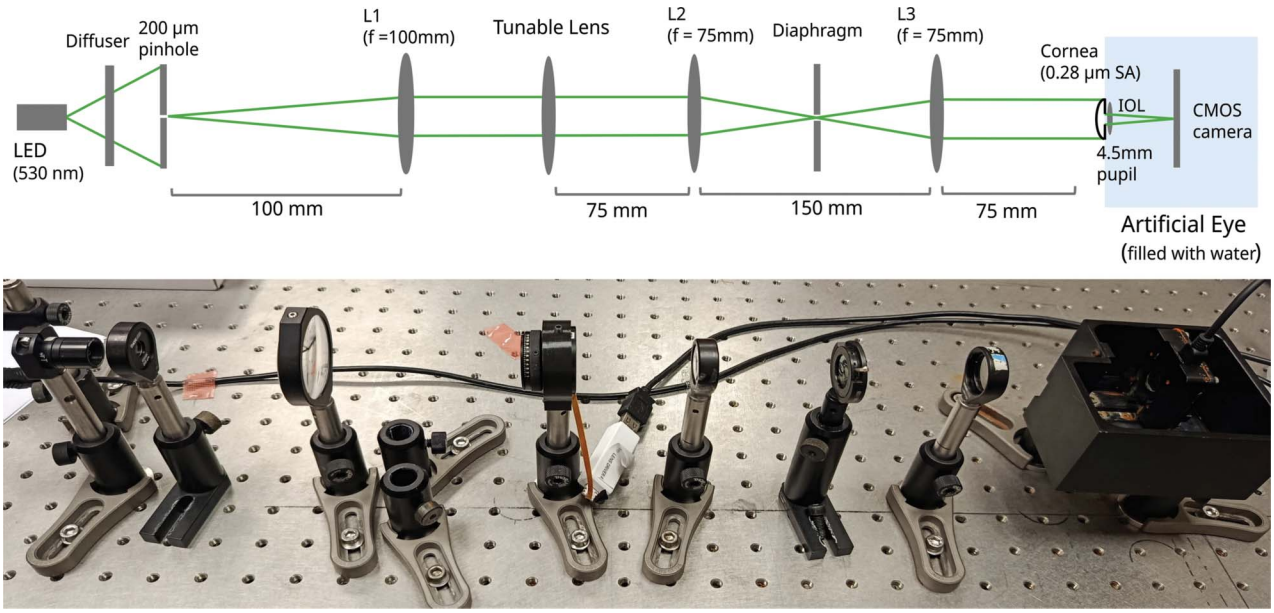

Figure 1. Schematic system setup consisting of an artificial eye with physiological cornea, IOL, and camera immersed in water. A tunable lens was conjugated with the spectacle plane to induce different object vergences. The bottom figure presents the real setup.

of the intensity was calculated for each image (ie, corresponding slice of the matrix). Considering that these IOLs are symmetrical, by calculating the radial average of the intensity for each object vergence and merging them all together, the cross sectional average of the 3D image of the pinhole can be retrieved.[24]

Different metrics were used to achieve a quantitative analysis of the images. The energy efficiency is widely used for the study of image formation in IOLs, and it can be defined as the ratio of energy encapsulated in a certain region of the image, I_R, to the total energy of the image, I_T.[25,26] As the energy incident on a pixel is proportional to its gray level, the energy contained in an area can be calculated by integrating the gray level (g) of the pixels in that area,

$$\eta_R = \frac{I_R}{I_T},\ I_R = \sum_{i=1}^{N} g_i$$

Considering that definition, the image can be divided into 3 areas with different associated efficiencies: the focused spot (η_F), the halo (η_H), and the peripheral residual noise (η_N). This definition is used to establish a threshold to find the halo size. The peripheral residual noise was taken as the area with the minimum gray level in the image. The maximum halo radius was considered as the position where the efficiency reached $\eta_{H+F} = 1 - \eta_N$. This calculation was performed for all object vergences.

In addition, the far focus images (or 0 D object vergence) were analyzed on their own, so the images were normalized separately. The radial average of the intensity, the halo radius, brightness, and relative halo magnitude (RHM) were compared across IOLs in this situation.[15,27] To calculate halo brightness, the Canny edge detection algorithm was used in the normalized HDR images to detect the extent of the focused image, and its mean radius was calculated (Figure S1, available at http://links.lww.com/JRS/B558). The mean brightness of the halo alone was determined as the average intensity between the focused spot edge and the halo radius. Given that the intensity of these images was normalized, the mean brightness calculated here is relative to the central intensity.

The RHM was also calculated for comparison. This metric uses the area under the curve of the logarithm of the normalized intensity to assess with a single quantity the size and brightness of the halo.

RESULTS

For zero object vergence, the obtained HDR images are presented in Figure 2 after a logarithmic transformation for better visualization of the halos. The normalized images, without the logarithmic transformation, can be found in the supplementary material (Figure S1, available at http://links.lww.com/JRS/B558).

It can be observed that the diffractive trifocal lenses produce larger and brighter halos, while the other IOLs display more diffuse light. Among nondiffractive lenses, EDOF and FVR exhibit more straylight compared with monofocals.

The normalized intensity plot of all the IOLs is shown in Figure 3, being the intensity in logarithmic scale. The distribution of light is remarkedly different for the diffractive trifocals than for the rest of lenses tested, including the refractive FVR IOLs.

The calculated data of halo size, brightness, and RHM for each IOL are summarized in Figure 4. Regarding size, the biggest halo is presented by AT Lisa (1.22 degrees), followed by FineVision (0.87 degrees) and PanOptix (0.84 degrees). The FVR lens, ArtIOL Art70, has a halo size of 0.63 degrees. The size of the halos produced by monofocal, enhanced monofocal, and EDOF has a similar magnitude, between 0.40 degrees for Tecnis ZCB00 and 0.48 degrees for Vivity. The lowest mean brightness (relative to the center) is presented by ArtIOL Art40 (0.019) and the highest associated with PanOptix (0.051) and the diffractive lenses. The rest of IOLs produced halos with mean brightness around 0.03 and 0.035.

The RHM parameter, as a global indicator of halo magnitude, is in good agreement with the halo size and

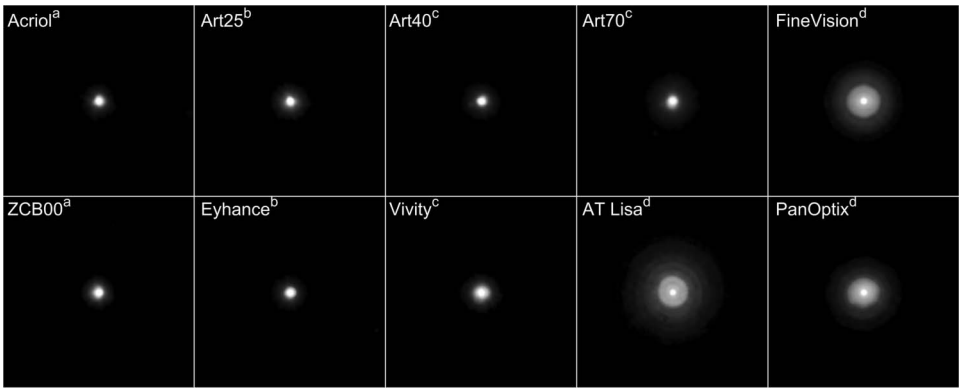

Figure 2. Obtained HDR images of the tested lenses. To enhance the visibility of the halos, the logarithm of the intensity is represented. The images are cropped to 4-degree retinal size. *a*: Monofocal, *b*: enhanced monofocal/monofocal plus, *c*: EDOF, *d*: diffractive multifocal IOLs. HDR = high dynamic range

brightness calculations. As the size and brightness of the halos increases, the RHM is bigger. Thus, diffractive lenses display higher values while monofocal and enhanced monofocal IOLs display the lowest. For some lenses, the RHM value is similar, such as ArtIOL Art70 (73.2) and Vivity (69.9), but have different halo characteristics. Art70 has a bigger but fainter halo, while Vivity has a smaller but brighter halo.

Figure 5 presents the cross-sectional rotational average of the HDR images in logarithmic scale of intensity, thus representing the through focus performance of the lenses. The dots represent the halo size, obtained as described previously. The figures without the logarithmic transformation can be found at the supplementary material (Figure S2, available at http://links.lww.com/JRS/B558).

Monofocal lenses share a common behavior, with the image increasing in size (getting blurred) rapidly with added object vergence, that creates a characteristic conic shape. EDOF lenses seem to maintain a narrower center (this is, a focused or less blurred image of the pinhole) throughout a wider defocus range. However, the conic shape is maintained, halos not being heavily present. For ArtIOL Art70, the situation is similar, but in its case, the halo is bigger and dimmer. AcrySof Vivity exhibits a more pronounced ring-like structure for high-vergence values than other EDOFs. For the diffractive trifocals, the focused spot is maintained over a wider range (it is more apparent in Figure S2, available at http://links.lww.com/JRS/B558), but the halos are present throughout the whole range of object vergence tested. The shape of the cross-section is therefore no longer conic, and the halo structure is relatively constant for all distances. In the case of PanOptix and AT Lisa Tri, there seems to be a slight decrease in halo size corresponding to the intermediate focus, but it is not that evident for FineVision.

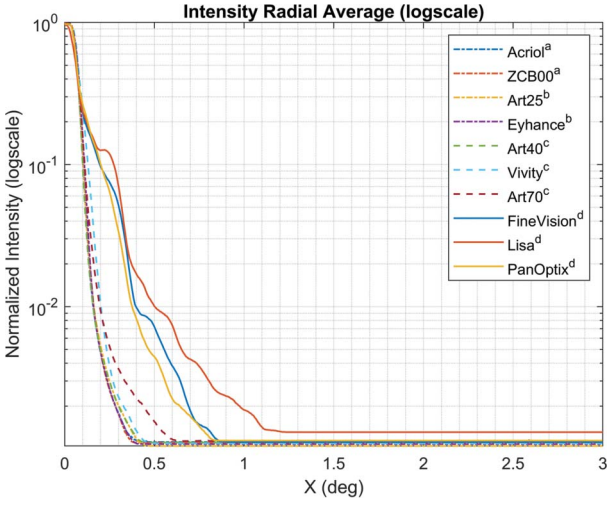

Figure 3. Average intensity profiles of all the lenses measured, in logarithmic scale. The intensity, on the vertical axis, is normalized. The horizontal axis represents the distance from the center of the image, until 3-degree retinal size. [a]Monofocal, [b]enhanced monofocal/monofocal plus, [c]EDOF, [d]diffractive multifocal IOLs.

DISCUSSION

We assessed the halo formation and through focus performance of 10 types of IOLs that comprised 2 monofocals, 2 enhanced monofocal/monofocal plus, 3 nondiffractive EDOF and FVR, and 3 diffractive trifocal lenses. As expected from the nature of the lenses studied, the results show that diffractive trifocal lenses present more structured halos, bigger in size and brighter. Enhanced monofocal and EDOF lenses behave similarly to a monofocal lens, and halo magnitude increased as the intended depth of focus increased as well. This is evident in the case of ArtIOL lenses, which increase depth of focus by inducing different amounts of negative SA. As the induced SA increases, both the magnitude and size of the halo also increase, with Art25 and Art40 having the smallest halo, and Art70 having the largest. The small difference in performance between Art25 and Art40 can be due to the amount of SA that each of them induced, and the extent to which corneal SA was compensated.

Regarding the through focus performance, the difference between diffractive and nondiffractive lenses is very apparent. Diffractive lenses maintained a consistent halo pattern across the entire range (with a slight reduction in the middle focus), whereas nondiffractive IOLs exhibited a conical shape, with a narrow region around the focused image at far that expands as defocus increases (near distances). This implies that diffractive lenses have the potential to produce halos at all distances. Conversely, nondiffractive IOLs, including both EDOF

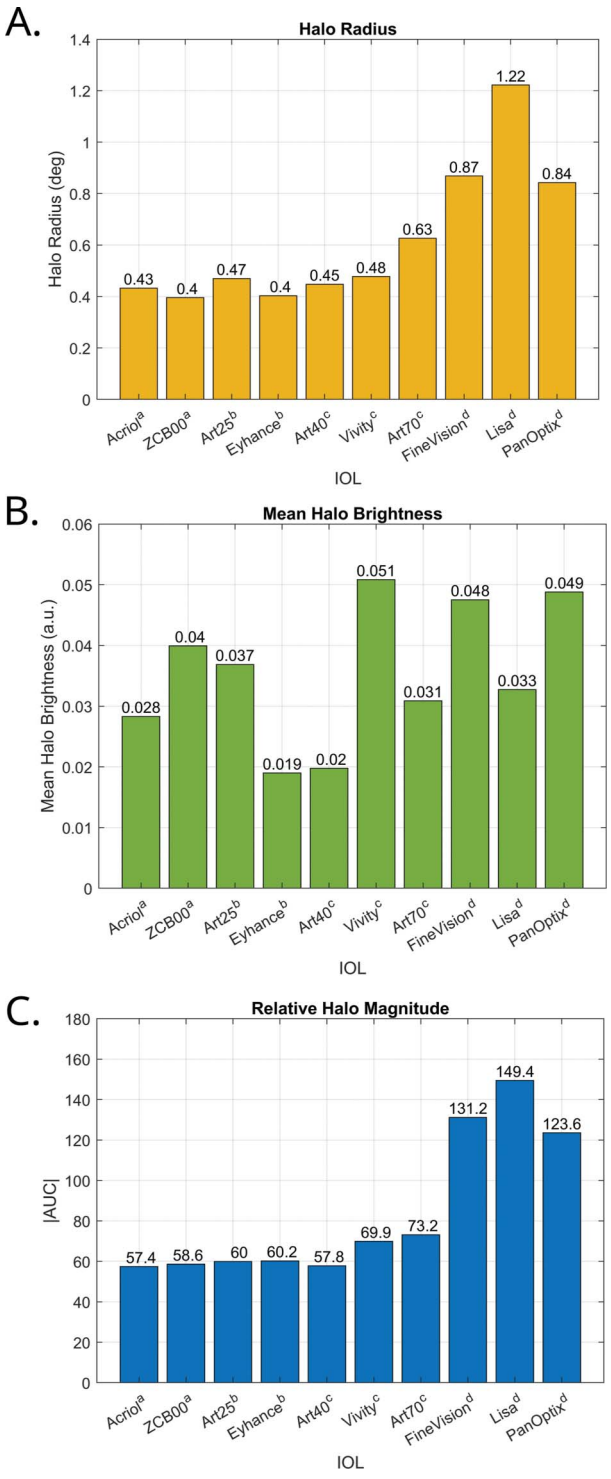

Figure 4. Metrics to evaluate the halo, calculated as explained in the Methods section. *A*: Halo radius in degrees. *B*: Mean halo brightness (a.u.). *C*: Relative halo magnitude (a.u.). [a]Monofocal, [b]enhanced monofocal/monofocal plus, [c]EDOF, [d]diffractive multifocal IOLs.

and monofocal, generally produced a minimal halo at best focus, while, at near distances, blur dominated optical quality.

For multifocal lenses, additional factors such as add powers and the effective diameter contributing to each focus also influence halo size.[3] In this study, all the multifocal lenses had diffractive structures up to 4.5 mm and partially compensated for corneal SA, but their diffractive designs differ: AT Lisa features a nonapodized diffractive trifocal center and bifocal peripheral zone, PanOptix uses a nonapodized trifocal design, and FineVision has an apodized trifocal design. These differences influence the energy distribution among foci and can account for the variation in shape and intensity of the halos observed in Figure 5.

Previous on-bench studies that included these lenses found that AT Lisa had the biggest halo, followed by FineVision and PanOptix.[27,28] This is in good agreement with the results found in this study, where the same trend persisted in both RHM and halo size. After the trifocals, the FVR Art70 and EDOF Vivity followed. The difference between the RHM results presented in this study and those of the bibliography, where higher RHM values are reported, can be due to the limited dynamic range of the camera used, the limited exposure values chosen to generate the HDR images, and the different units of intensity used to assess.[21] Although the values obtained here are lower, the relative differences between lenses remain consistent.

These results also concur with questionnaires on quality of vision. The lenses displaying more intense halos are the ones where patients reported the presence of halos more frequently. For AT Lisa, around 80% of patients perceived some level of halos (although 75% reported not being bothered by them); PanOptix and FineVision have shown similar values, with near 60% of patients having experienced halos to some degree (although FineVision performed slightly worse, no significant differences were found).[29,30]

Different methods of distributing light to create an extended depth of focus can result in different halo patterns. In general, as the light is more distributed to extend the focus, the halo will have lower intensity.[4] AcrySof Vivity presents a small but bright halo, while Art70 has a dim and larger halo, so there seems to be a compromise between halo brightness and size for these lens designs. In addition, Vivity displays a more defined ring-shaped halo structure for large object vergences. In a previous study, binocular implantation of Art40-Art70 showed that 96.4% of patients had never reported halos, while studies on the Vivity lens report that 60.4% of patients had never experienced halos and between 75.5% and 83% of them were not bothered by halos.[17,31,32] This suggests that brightness and through focus performance may play a decisive role in the subjective perception of halos.

Art25, Art40, and Eyhance's behavior was comparable with the monofocal IOLs, in both size, brightness, and RHM. These results agree well with other studies that have shown the superior image quality of enhanced monofocal lenses at intermediate distances and comparable in far focus to standard monofocals while not introducing additional photic phenomena.[33,34]

There were some limitations that should be acknowledged. First, the low dynamic range of the camera did not allow the calculation of absolute luminance values, and the

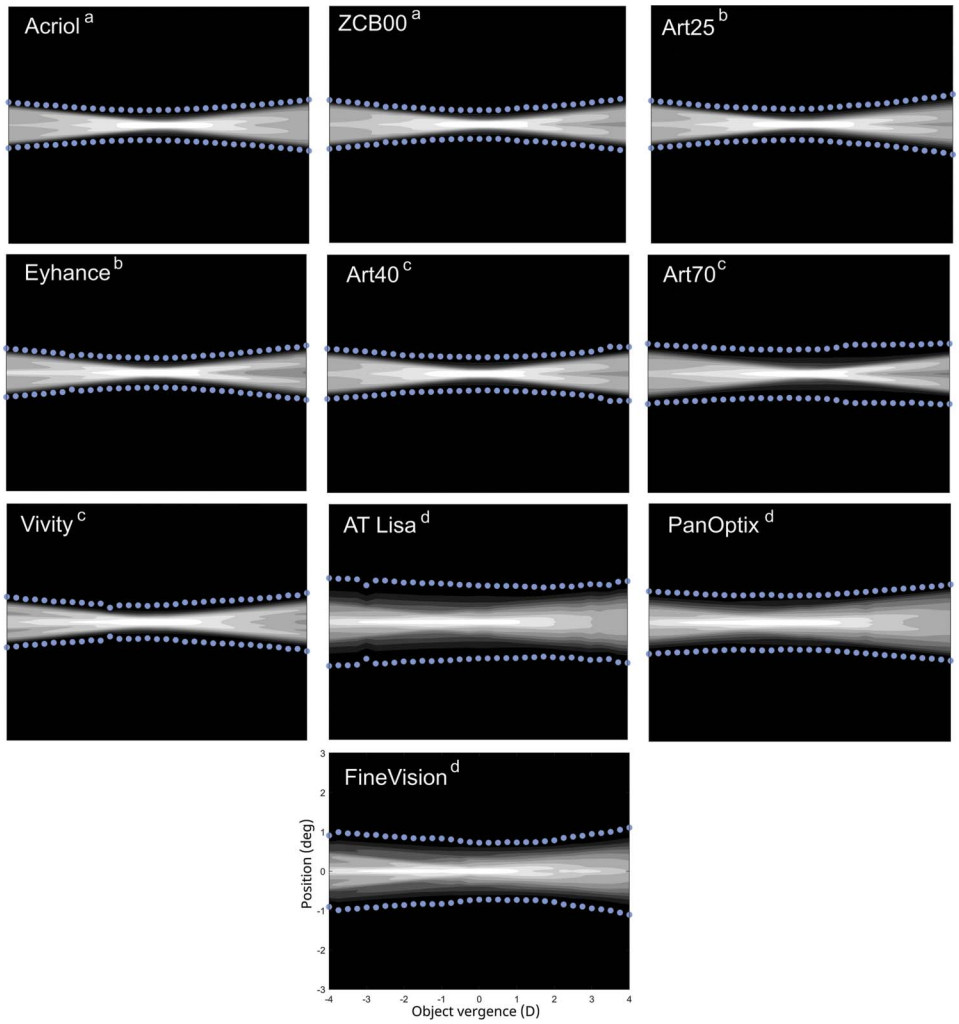

Figure 5. Cross-sectional average of the 3D point spread function (PSF). The intensity is represented in logarithmic scale for improved visualization. The horizontal axis represents object vergence, from −4 to 4 D in the spectacle plane. Distance from the center is on the vertical axis, from −3 to 3 degrees. The dots represent the halo size, as defined in the Methods section. [a]Monofocal, [b]enhanced monofocal/monofocal plus, [c]EDOF, [d]diffractive multifocal IOLs.

process of creating HDR images could introduce some artifacts. Second, experiments were performed under monochromatic light and just one corneal SA, future work could explore the effects of polychromatic light and different corneal SA on halo formation. Finally, the IOLs differed slightly in base power (19 to 22 D), which can affect retinal magnification and potentially benefit higher power lenses. To mitigate this, we converted retinal distances into subtended visual degrees for each IOL individually. In addition, raytracing simulations indicate that for an object of 1 degree, retinal magnification differences across this power range were small (5%). Since the through-focus comparisons were made qualitatively, we believe that these power differences do not compromise the validity of the conclusions.

Despite these limitations, the findings provide meaningful insight into the relative performance of the tested IOLs under a specific set of conditions.

In conclusion, in this comparative in vitro study, halo formation was assessed across 10 lenses with different designs. As expected, diffractive multifocal lenses produced larger halos compared with nondiffractive lenses. EDOF lenses behaved similarly to monofocal IOLs, although this varied depending on the amount of induced depth of focus. Inverted meniscus lenses performed as well as biconvex lenses and similar to other monofocal and EDOF lenses (Vivity and Eyhance). These findings contribute to existing knowledge and emphasize the value of in vitro measurements as a complementary tool to guide patients in choosing the most suitable IOL.

WHAT WAS KNOWN

- Diffractive multifocal IOLs have more intense photic phenomena associated with them.

WHAT THIS PAPER ADDS

- Comparison of monofocal, EDOF, and diffractive multifocal IOLs and their associated halos.
- Refractive EDOFs are closer to monofocal halo performance than to DMIOLs.
- Regarding halo formation, inverted meniscus lenses behave as well as biconvex IOLs of the same category, either enhanced monofocal (Eyhance) or EDOF lenses (Vivity).

REFERENCES

1. Pusnik A, Petrovski G, Lumi X. Dysphotopsias or unwanted visual phenomena after cataract surgery. Life. 2022;13(1):53. doi:10.3390/life13010053
2. de Silva SR, Evans JR, Kirthi V, Ziaei M, Leyland M. Multifocal versus monofocal intraocular lenses after cataract extraction. Cochrane Database Syst Rev. 2016; 2016(12):CD003169. doi:10.1002/14651858.CD003169.pub4
3. Alba-Bueno F, Vega F, Millán MS. Halos and multifocal intraocular lenses: origin and interpretation [in Spanish]. Arch Soc Esp Oftalmol. 2014;89(10): 397–404. doi:10.1016/j.oftale.2014.10.002
4. Alba-Bueno F, Garzón N, Vega F, Poyales F, Millán MS. Patient-perceived and laboratory-measured halos associated with diffractive bifocal and trifocal intraocular lenses. Curr Eye Res. 2018;43(1):35–42. doi:10.1080/02713683.2017.1379541
5. Yi F, Iskander DR, Collins M. Depth of focus and visual acuity with primary and secondary spherical aberration. Vision Res. 2011;51(14):1648–1658. doi:10.1016/j.visres.2011.05.006
6. Tabernero J, Otero C, Kidd J, Zahiño L, Noia A, Güell JL, Artal P, Pardhan S. Depth of focus as a function of spherical aberration using adaptive optics in pseudophakic subjects. J Cataract Refract Surg. 2025;51(4):307–313. doi:10.1097/j.jcrs.0000000000001608
7. Kohnen T, Berdahl JP, Hong X, Bala C. The novel optical design and clinical classification of a wavefront-shaping presbyopia-correcting intraocular lens. Clin Ophthalmol. 2023;17:2449–2457. doi:10.2147/OPTH.S400083
8. Artal P, Ginis H, Christaras D, Villegas EA, Tabernero J, Prieto PM. Inverted meniscus intraocular lens as a better optical surrogate of the crystalline lens. Biomed Opt Express. 2023;14(5):2129–2137. doi:10.1364/BOE.490089
9. Ginis H, Christaras D, Tsoukalas S, Artal P. Inverted meniscus IOLs prevent negative dysphotopsia. Invest Ophthalmol Vis Sci. 2024;65(7):6341
10. Lasch K, Marcus JC, Seo C, McCarrier KP, Wirth RJ, Patrick DL, O'Riordan JF, Stasaski R. Development and validation of a visual symptom–specific patient-reported outcomes instrument for adults with cataract intraocular lens implants. Am J Ophthalmol. 2022;237:91–103. doi:10.1016/j.ajo.2021.10.023
11. Lwowski C, Rusev V, Kohnen T. Assessment of visual habituation measured with the Halo & Glare Simulator and its impact on patient satisfaction following quadrifocal IOL implantation. J Refract Surg. 2023;39(8): 510–517. doi:10.3928/1081597X-20230612-01
12. Kohnen T, Suryakumar R. Measures of visual disturbance in patients receiving extended depth-of-focus or trifocal intraocular lenses. J Cataract Refract Surg. 2021;47(2):245–255. doi:10.1097/j.jcrs.0000000000000364
13. ISO 11979-2:2024. Ophthalmic implants-intraocular lenses: part 2: optical properties and test methods. Accessed January 30, 2025. https://www.iso.org/standard/86607.html
14. ANSI Z80.35-2018. Ophthalmics: extended depth of focus intraocular lenses. Accessed March 31, 2025. https://webstore.ansi.org/standards/vc%20(asc%20z80)/ansiz80352018?srsltid=AfmBOoo9tdPm-9-YKgiwNG9fjz3H9oX176q8_VM7B9aJyUKXZLB0xHW-
15. Carson D, Lee S, Alexander E, Wei X, Lee S. Comparison of two laboratory-based systems for evaluation of halos in intraocular lenses. Clin Ophthalmol. 2018;12:385–393. doi:10.2147/OPTH.S152201
16. Voptica SL. ArtIOLs Art 25. Accessed March 31, 2025. https://voptica.com/wp-content/uploads/2024/01/Voptica-Art25.pdf
17. Marín JM, Hervella L, Villegas E, Robles C, Alcón E, Yago I, Artal P. Visual performance at all distances and patient satisfaction with a new aspheric inverted meniscus intraocular lens. J Refract Surg. 2023;39(9):582–588. doi:10.3928/1081597X-20230802-01
18. Ginis HS, Tsoukalas S, Christaras D, Artal P. Visually relevant on-bench through-focus analysis of intraocular lenses. Biomed Opt Express. 2024; 15(12):7056–7065. doi:10.1364/BOE.540034
19. Togka KA, Livir-Rallatos A, Christaras D, Tsoukalas S, Papasyfakis N, Artal P, Ginis H. Peripheral image quality in pseudophakic eyes. Biomed Opt Express. 2020;11(4):1892–1900. doi:10.1364/BOE.387254
20. Guirao A, Redondo M, Artal P. Optical aberrations of the human cornea as a function of age. J Opt Soc Am A Opt Image Sci Vis. 2000;17(10): 1697–1702. doi:10.1364/JOSAA.17.001697
21. Wang L, Dai E, Koch DD, Nathoo A. Optical aberrations of the human anterior cornea. J Cataract Refract Surg. 2003;29(8):1514–1521. doi: 10.1016/S0886-3350(03)00467-X
22. Alba-Bueno F, Vega F, Millán MS. Design of a test bench for intraocular lens optical characterization. J Phys Conf Ser. 2011;274(1):012105. doi: 10.1088/1742-6596/274/1/012105
23. Reinhard E, Ward G, Pattanaik S, Debevec P. Chapter 4: HDR image capture. High Dynamic Range Imaging: Acquisition, Display, and Image-Based Lighting. San Francisco: Morgan Kaufmann; 2006:115–165.
24. Sievers J, Elsner R, Bohn S, Schünemann M, Stolz H, Guthoff RF, Stachs O, Sperlich K. Method for the generation and visualization of cross-sectional images of three-dimensional point spread functions for rotationally symmetric intraocular lenses. Biomed Opt Express. 2022;13(2):1087–1101. doi:10.1364/BOE.446869
25. Millán MS, Vega F, Ríos-López I. Polychromatic image performance of diffractive bifocal intraocular lenses: longitudinal chromatic aberration and energy efficiency. Invest Ophthalmol Vis Sci. 2016;57(4):2021–2028. doi: 10.1167/iovs.15-18861
26. Armengol J, Garzón N, Vega F, Altemir I, Millán MS. Equivalence of two optical quality metrics to predict the visual acuity of multifocal pseudophakic patients. Biomed Opt Express. 2020;11(5):2818–2829. doi:10.1364/BOE.388531
27. Kohnen T, Nouri SA, Carson D. Vehicle headlight halo simulation of presbyopia-correcting intraocular lenses. Transl Vis Sci Technol. 2023; 12(12):19. doi:10.1167/tvst.12.12.19
28. Carson D, Hill WE, Hong X, Karakelle M. Optical bench performance of AcrySof IQ ReSTOR, AT LISA tri, and FineVision intraocular lenses. Clin Ophthalmol. 2014;8:2105–2113. doi:10.2147/OPTH.S66760
29. Mendicute J, Kapp A, Lévy P, Krommes G, Arias-Puente A, Tomalla M, Barraquer E, Rozot P, Bouchut P. Evaluation of visual outcomes and patient satisfaction after implantation of a diffractive trifocal intraocular lens. J Cataract Refract Surg. 2016;42(2):203–210. doi:10.1016/j.jcrs.2015.11.037
30. Gundersen KG, Potvin R. Trifocal intraocular lenses: a comparison of the visual performance and quality of vision provided by two different lens designs. Clin Ophthalmol. 2017;11:1081–1087. doi:10.2147/OPTH.S136164
31. Bala C, Poyales F, Guarro M, Mesa RR, Mearza A, Varma DK, Jasti S, Lemp-Hull J. Multicountry clinical outcomes of a new nondiffractive presbyopia-correcting IOL. J Cataract Refract Surg. 2022;48(2): 136–143. doi:10.1097/j.jcrs.0000000000000712
32. McCabe C, Berdahl J, Reiser H, Newsom TH, Cibik L, Koch D, Lemp-Hull J, Jasti S. Clinical outcomes in a U.S. registration study of a new EDOF intraocular lens with a nondiffractive design. J Cataract Refract Surg. 2022; 48(11):1297–1304. doi:10.1097/j.jcrs.0000000000000978
33. Łabuz G, Son HS, Naujokaitis T, Yildirim TM, Khoramnia R, Auffarth GU. Laboratory investigation of preclinical visual-quality metrics and halo-size in enhanced monofocal intraocular lenses. Ophthalmol Ther. 2021;10(4): 1093–1104. doi:10.1007/s40123-021-00411-9
34. Wan KH, Au ACK, Kua WN, Ng ALK, Cheng GPM, Lam NM, Chow VWS. Enhanced monofocal versus conventional monofocal intraocular lens in cataract surgery: a meta-analysis. J Refract Surg. 2022;38(8):538–546. doi: 10.3928/1081597X-20220707-01

Disclosures: *C. García-Pedreño, J. Tabernero, H. Ginis, L. Hervella, and P. Artal have financial interests in Voptica SL.*

First author:
Clara García-Pedreño, MSc

Laboratorio de Óptica, Universidad de Murcia, Murcia, Spain